ABSTRACT

Shafts are frequently constructed to allow access to subsurface infrastructure and the resulting excavation generally deep and narrow. Shafts may be constructed using a variety of methods and plan forms dependent on ground conditions and intended use. An axisymmetric (cylindrical) geometry is often preferred due to the relatively simple structural analysis, construction method and for a number of approaches that are available to estimate the ground movements around such an excavation. In certain cases, particularly when there is restricted space both above and below surface, non-circular shafts could be a preferred solution. The assessment of surface movements around non-circular shafts is difficult as little information exists and there are few empirical prediction methods available. In this study, a series of centrifuge tests have been conducted to investigate the effects of modifying the cross-sectional profile of a shaft (i.e. circular in plan compared with elliptical). Analysis of measurements obtained from centrifuge tests undertaken at City, University of London's geotechnical centrifuge facility are presented and compared with existing predictive methods. An addendum to the empirical equations and procedures for predicting surface settlements arising from circular shafts is presented to allow for the assessment of movements around elliptical shafts in clay.

KEYWORDS

Shaft construction; Ground movements; Centrifuge modelling

LIST OF SYMBOLS

a	Constant indicates the depth at which maximum horizontal displacement occurs
b	Constant governs the height of the Gaussian curve
d	Distance from the shaft wall
D	Shaft diameter
H	Shaft depth
K_0	The ratio between horizontal and vertical effective stresses at rest
OCR	Overconsolidation ratio
n	Multiple of shaft depth, H, to a distance, d, from the shaft wall where settlement becomes zero
PIV	Particle Image Velocimetry
PPT	Pore Pressure Transducer
S_v	Vertical soil displacement
S_h	Horizontal soil displacement
S_u	Undrained shear strength of clay
α	Empirical constant
$\emptyset'_c$	Critical state angle of shearing resistance
σ'_h	Horizontal effective stress
σ'_v	Vertical effective stress
σ'_{v0}	Maximum consolidation pressure for clay model in centrifuge test
z	Depth below soil surface

INTRODUCTION

In a developed urban environment the surface space is heavily utilised leading engineers to develop tunnelling solutions for housing transport links, water services, sewage services, communication networks and electrical lines. Access to these tunnelling systems can be a considerable challenge, particularly for transportation systems where easy access is required for thousands of people daily. There are many solutions to this problem of access including the sinking of shafts to intersect with tunnels or other structures (such as stations) below. The construction of a deep shaft will generate ground movements driven by reduction of horizontal stresses on the soil around the shaft and vertical stresses at the base but also influenced by other factors such as method of shaft construction, workmanship and dewatering. In a dense urban environment these movements have the potential to cause structural damage to existing surface and subsurface infrastructure and this must be, at the design stage, assessed.

The most common geometric form of a shaft is circular in plan cross-section. This shape is favoured due to the inherent advantage of radial symmetry. In this case the analysis of the lining can assume that loads are carried by the stiff hoop and that any ground movements generated during construction will be radially symmetric both above and below the ground surface. These assumptions do not, of course, account for variations in the soil around the shaft or construction methods and tolerances (potentially leading to non-uniform pressures being applied to the lining and non-uniform ground movement) or the presence of any existing buildings which would also contribute to asymmetric behaviour.

In theory a shaft can be sunk with any cross-sectional geometry. There are obvious disadvantages to certain shapes (e.g. a square or rectangular shaft would require a stiff design at the corners of the lining to counter the bending moments generated by the pressure acting on the sides) but there are advantages to an elliptical cross-section particularly in cases of restricted surface space (e.g. Feiersinger, 2011). Figure 1 shows a sketch of a hypothetical project to install two lifts for underground access to a metro station. The lifts are represented by the squares and the required circular or elliptical shaft to house them is shown. For this particular (notional) geometry the elliptical shaft has a plan area that is approximately 25% smaller which would have significant benefit in terms of removal of spoil from site. Additionally, the elliptical geometry could

be aligned in such a way so as to avoid any surface or subsurface structures that may already exist. Taking into account these potential benefits, the objective of this paper is to provide experimental data on elliptical shaft construction in clay to support current design methodologies.

SHAFT DESIGN AND CONSTRUCTION

Construction of a shaft in clay can be carried using a number of methods dependent on the strength of the clay. Allenby & Kilburn (2015) discuss shaft-sinking techniques divided into two general categories; underpinning and caisson sinking however Schwamb (2014) also highlights the use of piling and diaphragm walling as viable construction techniques. In an urban environment where there are limitations on available space, noise and vibrations, shafts are usually constructed by underpinning (e.g. Morrison *et al.*, 2004). Underpinning is a construction technique which incrementally excavates the shaft followed by installation of a pre-cast concrete segmental lining and grouting behind the annulus (Allenby & Kilburn, 2015). There are also recent examples of shaft construction in stiff clays using a sprayed concrete lining (e.g. Rutty *et al.*, 2015) which also use an underpinning method. It is worth highlighting this technique as its flexibility would make it most suitable for construction of non-circular geometries. When utilising sprayed concrete, excavation is followed by construction of a primary lining (using sprayed concrete) which is then supplemented by a secondary lining constructed soon after (usually Cast-in-place or pre-cast concrete). The primary lining can be assumed to carry none of the load in the long term (as in Rutty *et al.*, 2015) or it can work with the secondary lining (as in Psomas *et al.*, 2019).

Modern geotechnical engineering practice aims to reduce ground movements arising from construction to a minimum. BS EN 1997-2:2007 (BSI, 2007) specifies that the design of a shaft (of any cross-section) must include detailed assessments of the adjacent ground movements in order to assess any impact on existing structures. There is little guidance available to aid with these assessments although, most notably, New & Bowers (1994) give a prediction method for surface settlements arising from circular shaft sinking in London clay (recently updated; New, 2017). In this work it is asserted that predictions can only be made by referring to field data in similar soil conditions but these data are relatively limited in the literature, particularly so when compared with those of other geotechnical construction events (i.e. tunnelling). Le *et al.* (2019)

extends this work to subsurface movements but again, the field data with which to validate these methods is limited.

When considering an elliptical shaft, it may be possible to adapt the work of New (2017) with additional modifications or assumptions in order to generate surface settlement predictions. Alternatively, finite element methods could be used to make predictions of ground movements (e.g. Pedro *et al.*, 2019) but observational data are vital for validating any numerical analysis of elliptical shaft excavations. There are very few published case studies reporting the construction of and the ground movements arising from elliptical shafts. Feiersinger (2011) reports the construction of a lift shaft at Green Park station in London using a sprayed concrete primary lining and cast-in-place secondary linings and whilst some information is given on instrumentation that was installed for surface movements, the measurements reported concentrate on the influence of the shaft on existing subsurface assets such as escalators and tracks. The shaft is approximately 27m deep with a major and minor axis of 8.6m and 5.6m respectively in the upper 10m widening to a major and minor axis of 10m and 6.2m for the remaining depth. Topa Gomes *et al.* (2008) report a shaft construction based on two overlapping ellipses in a relatively uncongested urban space. Some subsurface movements are presented but relatively close to the shaft walls. In general, there is a lack of reported case data on which to base future assessments.

GROUND MOVEMENTS ARISING FROM SHAFT CONSTRUCTION

Ground movements generated by shaft construction will comprise vertical settlements and horizontal movements towards the shaft. These are primarily driven by reductions in horizontal and vertical earth pressures however, as Faustin (2017) identifies, there are many factors that contribute to the overall movements both in the short and the long term. These include (but are not limited to) the diameter and depth of the shaft, the construction method employed, workmanship, ground conditions and other processes such as dewatering or consolidation.

The vertical surface settlements arising from sinking a circular shaft in stiff London Clay during the Heathrow Express Trial Tunnel were reported by New & Bowers (1994) and used to establish **Equation 1**.

$$S_V = \alpha H \left(1 - \frac{d}{H}\right)^2 \quad (1)$$

Where S_V is the surface settlement at a distance, d, behind the wall. H is the depth of shaft and α is an empirical constant that depends on ground conditions and construction method (in the original work α had a value of 6×10^{-4}). The limitations of **Equation 1** are that the diameter of excavation is not considered and there is a level of uncertainty surrounding the value of α.

Subsequently, New (2017) documented field data from thirteen case studies with a wide range of diameters (although predominantly in stiff London Clay). An amendment to **Equation 1** was proposed with a new variable, *n*, controlling the extent of the vertical settlements around the excavation (**Equation 2**).

$$S_V = \alpha H \left(1 - \frac{d}{nH}\right)^2 \quad (2)$$

Whilst there is still no explicit term considering the diameter of the shaft, the data presented by New (2017) clearly shows that larger shafts produce (as might be expected) larger settlements over a greater extent. It might also be logical that softer soils would produce larger movements, an observation supported by the experimental data from Le *et al.* (2019).

As noted earlier, there is limited published data in the literature reporting either field measurements, experimental data or numerical analyses of shaft construction. When considering elliptical shafts the available literature is even more restricted however, Faustin e*t al.* (2018) report a series of centrifuge tests on model elliptical shaft excavations in sand. These tests modelled a 1:80 scale elliptical shaft excavation (with equivalent prototype dimensions of major axis length = 14.4m, minor axis length = 9.6m and excavation depth 15.4m) in Fraction E Leighton Buzzard Sand with a stiff aluminium liner. The measurements during these tests were of the surface settlement and lining strains. The surface settlement data was compared with those from tests on circular shafts and showed that the maximum settlement was slightly higher in the elliptical shaft excavation (0.028%H compared with 0.02%H). However, it should be noted that these measurements may not be directly comparable as the plan area of the elliptical shaft modelled is larger than that of the circular shaft. Faustin *et al.* (2018) also state that the extent of the surface settlements is larger for the circular shaft when compared with the elliptical shaft (1.5H compared

with 1.0H) however the data presented do not necessarily support this rather more measurements are reported for the circular tests at a greater distance from the shaft.

It is clear that, accepting that elliptical shaped shafts are likely to be utilised in future construction projects, there is a need to understand and predict the movements generated during their excavation. A series of centrifuge tests to examine this are now described.

CENTRIFUGE TESTING

Novel apparatus was developed to model the ground movements induced by a circular shaft excavation in overconsolidated clay (Divall & Goodey, 2016). In that work, good agreement was shown between the data collected from experiments using this apparatus and the prediction methods of New (2017). This apparatus does not model the soil-structure interaction between the soil and the shaft liner but rather it generates ground movements by allowing a small gap between the soil and a solid former to close, analogous to the volume loss that might be observed during tunnel excavation. The rationale for this experimental approach is to remove any influence of liner stiffness and concentrate solely on the patterns of ground movement. Based upon the designs described by Divall & Goodey (2016), modifications were made to the apparatus for modelling elliptical shafts whilst using an identical test procedure.

Test apparatus

A basic apparatus schematic of the shaft centrifuge models is given in Figure 2. In this series of experiments, all excavations are modelled as half-space simulations. This allows measurements of soil movement to be made using digital analysis of images taken of the experiment through a Perspex window on one side of the container. This would not be possible if the experiments utilised a full model of the shaft. The finished model comprises a consolidated clay sample with a pre-cut excavation, into which is placed an apparatus supporting that excavation during in-flight consolidation which then allows simulation of the shaft construction once the groundwater conditions are established.

The apparatus comprises a fully solid former enclosed within a latex bag. This solid former is used instead of a thin hollow liner to support the soil in its final position as, in these experiments

where only half of the shaft is modelled, use of a thin liner would incorrectly represent the boundary condition at the edges in the plane of the cut. At the very base of the former, there is a small cavity which allows for basal heave to develop as the vertical stress is relieved during the excavation simulation. In this area the former is more representative of the real case but the wall is sufficiently thick to minimise bending. This apparatus is suspended from a stiff bracket attached to the upper surface of the box containing the experiment. The former is sized such that when installed within the pre-cut shaft excavation, there is a 4.5mm annular gap between the clay and the outer face of the former. The latex bag has a thickness of 1.5mm and, as such, when assembled there is a uniform 3mm gap around the annulus of the model. This gap can be considered to represent the amount of overcutting that might occur during excavation and the former to be the final position of the (e.g.) precast shaft lining. Thus, in the experiment, movements are driven by the closing of this annular gap. The amount of overcutting modelled here (300mm at prototype scale) is relatively large (100mm might be expected in practice). The choice of a 3mm gap is driven by the need to generate movements large enough to measure however the resulting measurements are normalised for comparison with other experiments or case studies. The void between former and latex bag (which includes the cavity at the base) is filled with a heavy fluid (sodium polytungstate) which has a bulk unit weight equivalent to that of the surrounding soil. This heavy fluid supports the clay both around the shaft and at the formation level during centrifuge flight whilst the pore pressures in the soil reached hydrostatic equilibrium with a water table set by a standpipe (at the ground surface) outside the model. Simulation of construction is then effected by draining the heavy fluid from the base of the latex bag which simultaneously reduces the horizontal stresses at the shaft perimeter and the vertical stress at formation level. Figure 3 shows the apparatus, how it sits within the clay model and how it attaches to the box within which it sits. More details of the model apparatus setup (for the reference case circular shaft geometry) are given in Le *et al.* (2019).

The two model elliptical shafts (shown in Figure 2) had plan cross-sectional areas equal to the circular shaft which is used as a reference case and is of the same dimensions as that described by Le et al. (2019) which is of 8m diameter and 20m depth at prototype scale, but had major and minor axes chosen to represent an approximately similar aspect ratio to the lower section of the elliptical shaft constructed at the Green Park underground station upgrade in London, UK

(Feiersinger, 2011). The tests were conducted at 100g and thus the model elliptical shaft had a minor axis of 64mm, a major axis of 100mm and a depth of 200mm, the slight variation between this and the prototype size being due to the requirement of the plan area being the same as the circular reference case. It should be noted that both apparatus representing the elliptical shafts have the same dimensions but have their plane of symmetry (in the model) corresponding with either the major or the minor axis. This approach allows a modelling of models scenario and enables investigation of the two different ground movement measurement techniques (detailed later).

Test series

A total of three tests were completed during this work. All three clay samples used in the tests were consolidated to 350kPa and swelled to 250kPa. All samples underwent further in-flight consolidation on the centrifuge resulting in samples that had varying strength and overconsolidation ratio with depth. The tests can be separated into two categories; CR, the reference circular shaft simulation and EL1 & EL2, the two different elliptical shaft simulations. Details of these test are summarised in Table 1. Where H is the depth of excavation, h is the horizontal axis length (i.e. the dimension across the box), v is the vertical axis length (the dimension into the box) and A is the cross-sectional area of the model shafts.

Test procedure and instrumentation

The soil samples were created by mixing Speswhite kaolin powder, a clay whose engineering properties are well-established for centrifuge modelling (Grant, 1998), with distilled water to a form a slurry with a water content of 120% (twice the liquid limit). This slurry was placed within a soil container, known as a strongbox, and subjected to a vertical effective stress history as detailed previously. This process took approximately one week. During the swelling stage, two pore-water pressure transducers were installed via the back wall of the strongbox, the primary function of which is to ensure that pore water pressure within the soil achieves equilibrium with the standpipe during the in-flight consolidation phase.

Once the clay sample is prepared, the model making procedure would begin more details on which can be found in Le *et al.* (2019). The main aspects are briefly described below:

- The front wall of the strongbox was removed and the exposed surfaces of the clay sample were sealed with silicone oil to prevent drying out,
- The soil sample was trimmed to the desired model height (275mm) and the semi-elliptical/circular cavity was manually cut into the front face of the clay sample using a specially constructed cutter and guide,
- This front face of the model was sprayed with dyed blue Leighton Buzzard Sand (Fraction B) whereas the top of the model was sprinklered with Leighton Buzzard Sand (Fraction E) to create the texture necessary for post-test image analysis of soil movement,
- The 83mm thick PMMA (Poly(methyl methacrylate)) window was bolted to the front of the strongbox which had the model shaft elements already attached,
- The drainage channels were connected and the gantry necessary for 3D topography (Le *et al.*, 2016) was bolted to the top of the strongbox (Figure 3), and finally,
- The latex bag was filled with the heavy fluid and all air bled out of the system.

The model was placed on the centrifuge swing (City, University of London has access to an Acutronic 661 and a description of the main features can be found in Panchal, 2018) and accelerated to 100*g*. The model was kept at this acceleration until the clay had reached hydrostatic equilibrium indicated by the stable readings from the aforementioned pore-water pressure transducers.

Simulation of the excavation process was achieved by draining the heavy fluid from the void between the former and latex bag. The rate of flow of the heavy fluid was set such that the entire process took approximately three minutes. Data from the surface displacements, subsurface displacements, pore-water pressure and heavy fluid pressure was taken at a rate of one per second. Once all ground movements had stopped the model was decelerated and hand shear vane readings were taken at various depths within the clay outside the zone of influence of the shaft. These readings could be used to determine the undrained shear strength, S_u, for each model. McNamara et al. (2011) demonstrated that, in this type of overconsolidated clay sample, post-test shear vane readings taken in the far field provided measurements of S_u directly comparable with in-flight measurements using a penetrometer and these readings are therefore

considered representative of the initial undrained shear strength of the sample. These results can be found in Figure 4 along with the calculate variation in OCR.

RESULTS

Correlation of test data

Before any comparison of settlement data can be undertaken, it is necessary to ascertain the similarity between each model. Aside from the differences in geometry, there are other experimental factors that may influence the results obtained such as inconsistencies in undrained soil strength and initial fluid level within the excavation (i.e. the horizontal pressure supporting the soil around the shaft). The best fit lines to the measurements of undrained shear strength shown in Figure 4 indicate that Test CR and EL1 show very similar undrained strength profiles (with some expected scatter in the discrete readings) whereas Test EL2 is somewhat lower. For example, at a depth of 100mm (i.e. half the depth of the shaft) the undrained strength of EL2 is approximately 10% lower than CR and EL1. Pressure measurements within the heavy fluid also showed that the initial fluid level within the excavation was around 20% higher in Test EL2 compared with that in Tests CR and EL1. These differences in initial conditions arise from the complex nature of the apparatus and model preparation process but will clearly have an effect on the measured results.

It is necessary to separate the effects on ground movements of these experimental variations from the differences that arise from changing the geometry of the shaft and a method was devised to account for the overall influence of the experimental variations. The presence of the stiff former implies that the end position of the soil is known i.e. once the fluid is drained, the soil moves (generally) horizontally until it comes into contact with the former. The effect of experimental differences can therefore be quantified by measuring the horizontal movement of the soil immediately adjacent to the shaft former as the fluid is drained. This movement must represent the distance between the soil's initial position and the former. Figure 5 shows this data, obtained from digital image analysis using geoPIV_RG (Stanier *et al.*, 2015). It is clear that the horizontal movements in test EL2 are larger, indicating a bigger initial gap which is considered to be the dominant factor in the measured surface movements upon excavation. The area under each

curve was obtained by numerical integration and it was found that (considering Test CR as the reference case) test EL1 had horizontal movements that were 3% lower than the reference case and test EL2 has movements that were 54% higher. This measurement can be considered to be analogous to the concept of volume loss used in tunnelling. The rate of excavation in the test is high and the event is essentially undrained. As such, the data for each test can be normalised to account for the fact that the movements driving the observed mechanisms (i.e. the initial gap between soil and former at the end of in-flight consolidation) are greater or smaller than the circular reference case.

Accounting for the effect of friction at the clay model and PMMA window interface

In this paper, measurements of soil movements are presented from various areas of the model and comprise surface settlement measurements obtained from 3D topography (Le *et al.*, 2016) and front face, subsurface measurements from geoPIV_RG (Stanier et al, 2015). Le *et al.* (2016) demonstrated that both of these techniques were capable of making measurements with comparable degrees of precision and accuracy. The (necessary) use of different measurement techniques means that come correlation must take place as front face measurements obtained from digital image analysis are influenced by friction between the soil and front window of the strongbox. Grant (1998) examined this phenomenon in a series of experiments using clay samples prepared in an identical manner to those in the current work and determined that an offset of -0.1 mm was evident in the region of interest when comparing results from LVDTs and image analysis. Put another way, Grant (1998) accounted for the friction at the clay-window interface by adding 0.1 mm to the settlements taken from digital image analysis.

In the current work, the region of interest is larger than that considered by Grant (1998); his work considered the movements immediately above a tunnel excavation. The application of an offset was therefore deemed inappropriate in this case. The reported 0.1 mm correction of Grant (1998) correlates to a scaling of around 10% and this scaling factor was therefore applied to measurements made at the clay-window interface in the work presented here.

To summarise, all results obtained (i.e. from both measurement systems at all locations) were scaled to account for variations in the experimental technique as previously detailed.

Subsequently, measurements made at the front face of the model were increased by 10% to account for interface friction.

Surface settlement data

Once the corrections detailed above have been applied to tests EL1 and EL2 it is possible to compare the surface settlements obtained parallel to the major and minor axes of the elliptical shaft and compare them with the (axisymmetric) settlements generated by the circular shaft. Figure 6 shows a sketch of the location of the measurement points and Figures 7a and 7b show the comparison along the major and minor axes respectively. In these figures it should be noted that those data labelled “P” (solid markers) are taken perpendicular to the front face of the centrifuge strong box using 3D topography and those labelled “F” (open markers) are taken at the front face both by geoPIV_RG and 3D topography (hence the larger number of data points).

The dashed lines are least squares best fits of Equation 2 to the data from the circular reference test and the elliptical shaft tests. Data from the elliptical tests show good agreement independent of the measuring technique used. Settlements along the major axis are significantly smaller than those generated by the circular shaft excavation despite the major axis being 25% larger than the diameter of the circle (100mm vs 80mm). Conversely, settlements along the minor axis are comparable with those generated by the circular excavation despite the minor axis being 20% smaller than the diameter of the circle.

DISCUSSION

The nature of the modelled shaft

It should be noted that the normalised settlements presented from the current tests are very much larger (by an order of magnitude) than those observed in the field (New, 2017). This arises from the fact that, in these tests, there is a 300mm overcut (at prototype scale) between the soil and the permanent former. As previously discussed, this is very much larger than that which might be encountered in practice where a 100mm overcut that is subsequently grouted might be more reasonable. The large overcut is an artifact of the experiments deliberately chosen to ensure consistent movements that can be reliably detected by digital image correlation.

The heavy fluid within the excavation is drained via a pipe embedded within the soil attached to the base of the latex bag. It might be expected that the presence of this pipe would have some influence on the ground movements however it is located on the centreline of the excavation. As this is also aligned with a plane of symmetry, movements in this area would be expected to be in the form of vertical heave only and would be less influenced by the smooth pipe, in itself aligned with the direction of heave. Post-test inspection shows that the pipe and latex bag have very little effect on the heave at the formation and what influence there is occurs only when the soil is fully softened at the base i.e. some time after the end of excavation simulation.

Comparison with empirical methods

Figure 8 shows that the surface settlements generated by the elliptical shaft excavation could be represented by Equation 1 (New, 2017). A least squares best fit to the combined data (i.e. from all tests and measurement methods) is carried out to determine values of α and n. Figure 8 shows the resulting curves and Table 2 gives the derived values of α and n.

Comparison with the results of Faustin et al. (2018)

As detailed earlier there is one previously published set of experimental data detailing a centrifuge test on an elliptical shaft constructed in dense sand. Despite the differences between this and the current work, Equation 2 is utilised to examine the patterns of movement generated. Figure 9 shows the results from Faustin *et al.* (2018) overlain with predicted curves generated by Equation 2. The curves are not mathematically fit to the data but rather placed to give an approximate upper bound to the data on the graph. The curve generated for the elliptical data has a value of α that is 10% larger than that used for the circular curve (the value of *n* is constant at 1.5). This is commensurate with the observation that the plan area of the elliptical shaft is 10% larger in this work when compared with the circular. The curves give credence to the observation above that a suitable prediction can be generated for the maximum settlements caused by excavating an elliptical shaft from Equation 2 by considering a circular shaft of equivalent plan area. It should be noted that in the current work, the aspect ratio of the ellipse is 0.64 (and 0.67 in Faustin *et al.*, 2018). Whether similar patterns of settlement would be observed for different aspect ratios remains a topic for future work.

CONCLUSION

A practical solution to the problem of restrictions on available surface space coupled with increasingly congested underground space is the utilisation of elliptical shafts for access to underground infrastructure. It is clear that there is a requirement for estimating the ground movements resulting from such constructions and data from a series of well-controlled centrifuge tests carried out in overconsolidated clay have been presented in this paper.

The findings can be summarised below:

- The maximum settlements at the ground surface arising from elliptical shaft construction are apparent on line coincident with the minor axis of the ellipse. Conversely, the settlements generated on the line coincident with the major axis are significantly smaller in magnitude (in the order of 60% of the settlement seen on the minor axis, for the ratio in lengths of the minor to major axis of 0.64).
- For the purposes of assessing the movements that might be generated by a proposed elliptical shaft construction in clay, an upper bound to the surface settlements can be generated from Equation 2 by modelling a circular shaft of equivalent plan area. As with the original work of New & Bowers (1994) special consideration will still need to be given to an appropriate value of α.

ACKNOWLEDGEMENT

The authors gratefully acknowledge the support of the Leverhulme Trust (Grant no. RPG-2013-85).

REFERENCES

Allenby, D. & Kilburn, D. (2015) Overview of underpinning and caisson shaft-sinking techniques. Proceeding of the Institution of Civil Engineers – Geotechnical Engineering, Vol. 168, No. 1, pp. 3-15.

British Standards Institution (2007). BS EN 1997-2:2007 Euro-code 7: Geotechnical Design. Ground investigation and testing. BSI, London, UK.

Divall, S. & Goodey, R.J. (2016). An apparatus for centrifuge modelling of a shaft construction in clay. In L. Thorel, A. Bretschneider, M. Blanc, & S. Escoffier (Eds.), *3rd European Conference on Physical Modelling in Geotechnics (Eurofuge 2016)* Vol. 1 (pp. 307-312), Nantes, France.

Faustin, N.E. (2017). Performance of circular shafts and ground behaviour during construction. PhD Thesis, Cambridge University, Cambridge, UK

Faustin, N.E., Elshafie, M.Z.E.B. & Mair, R.J. (2018). Modelling the excavation of elliptical shafts in the geotechnical centrifuge. Proceedings of the 9th International Conference on Physical Modelling in Geotechnics, Vol 2, pp. 791-796. London, UK.

Feiersinger, A. (2011). Comparison of deformations predicted using 3D finite element analysis with deformations encountered during construction. The Harding Prize Competition, British Tunnelling Society.

Grant, R.J. (1998). Movements around a tunnel in the two-layer ground. PhD thesis, City, University of London, UK.

Le, B.T., Goodey, R.J. & Divall, S. (2019). Subsurface ground movements due to circular shaft construction. Soils and Foundations, Vol. 59, No. 5, pp. 1160-1171.

Le, B.T., Nadimi, S., Goodey, R.J. & Taylor, R.N. (2016). System to measure three-dimensional movements in physical models. Géotechnique Letters, Vol. 6, No. 4, pp. 256-262.

McNamara, A.M., Rettura, D., & Gorasia R.J. (2011). Press-In Engineering, Proceedings of 3rd International Workshop, Shanghai, pp 25-31.

406 Morrison, P.R.J., McNamara, A.M. & Roberts, T.O.L. (2004). Design and construction of a deep
407 shaft for Crossrail. Proceedings of the Institution of Civil Engineers – Geotechnical
408 Engineering, Vol. 157, No. 4, pp. 173–182.
409 New, B. (2017). Settlements due to shaft construction. Tunnels and Tunnelling International,
410 September 2017, pp. 16-17.
411 New, B.M. & Bowers, L.K. (1994) Ground movement model validation at Heathrow Express trial
412 tunnel, Tunnelling ’94. London, UK.
413 Panchal, J.P. (2018). Minimising ground movements around deep excavations in soft soils. PhD
414 Thesis, City, University of London, London, UK
415 Pedro, A.M. (2013). Geotechnical investigation of IVENS shaft in Lisbon. PhD Thesis, Imperial
416 College, London, UK.
417 Psomas, S., Coppenhall, P., Rimes, M., Brown, D. & Cheevers, E. (2019). Design and
418 construction of permanent steel fibre reinforced sprayed concrete lining shafts for the
419 Thames Tideway Tunnel project UK. Proceedings of the World Tunnel Congress 2019,
420 Naples, Italy.
421 Rutty, P., Bedi, A., Hsu, Y.S., Heath, I. & Mimnagh, F. (2015). Design and construction of a spray
422 concrete lined shaft adjacent to running tunnels. Proceedings of the 16th European
423 Converence on Soil Mechanics and Geotechnical Engineering, Vol. 2, pp. 509-514.
424 Edinburgh, UK.
425 Schwamb, T. (2014) Performance Monitoring and Numerical Modelling of a Deep Circular
426 Excavation. PhD Thesis, Cambridge University, Cambridge, UK.Stanier, S.A., Blaber, J.,
427 Take, W.A. and White, D.J. (2015). Improved image-based deformation measurement
428 for geotechnical applications. Canadian Geotechnical Journal, Vol. 53, No. 5, pp. 727-
429 739.
430 Topa Gomes, A., Silva Cardoso, A., Almeida e Sousa, J. Andrade, J. & Campanhã, C. (2008).
431 Design and behaviour of Salgueiros station for Porto Metro. Proceedings of the 6th
432 International Conference on Case Histories in Geotechnical Engineering, Vancouver,
433 USA.
434

LIST OF FIGURES

Test ID	Maximum consolidation pressure (kPa)	Swelling pressure (kPa)	Excavation dimensions (mm or mm^2)	Shaft liner dimension (mm or mm^2)
CR (aspect ratio = 1.0)	350	250	h = v = 80 H = 200 A = 5027	h = v = 71 H = 200 A = 3959
EL1 (aspect ratio = 0.64)	350	250	h = 64 v = 100 H = 200 A = 5027	h = 55 v = 45.8 H = 200 A = 3959
EL2 (aspect ratio = 0.64)	350	250	h = 100 v = 64 H = 200 A = 5027	h = 91.6 v = 55 H = 200 A = 3959

Table 1: Details of centrifuge tests

Test	**CR**	**EL1**	**EL2**
α	5.8×10^{-3}	4.1×10^{-3}	5.9×10^{-3}
n	1.5	0.94	1.33

Table 2. The values of α and n derived from the tests.

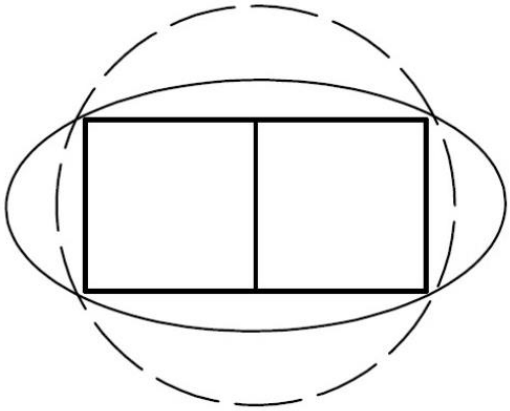

Figure 1: Sketch showing required circular and elliptical plan geometry to enclose two adjacent lift mechanisms**.**

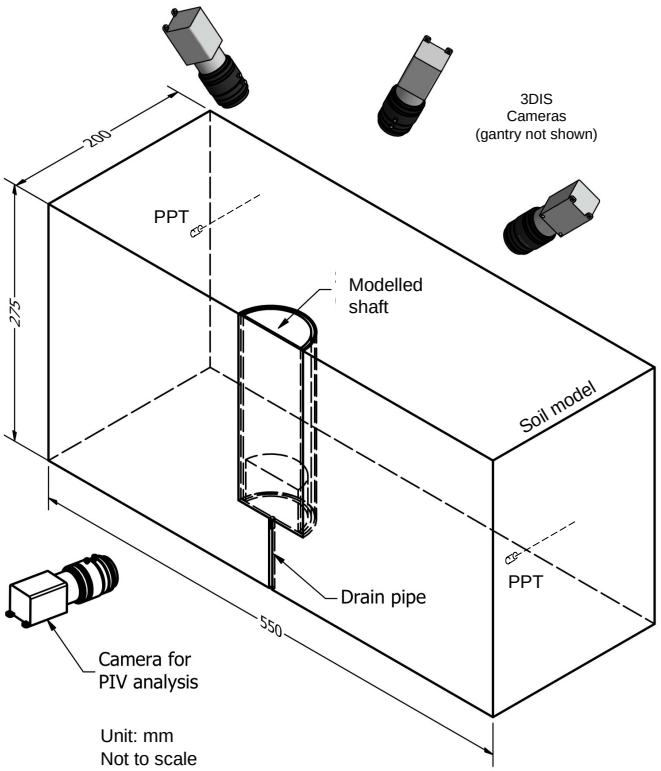

a) Test apparatus

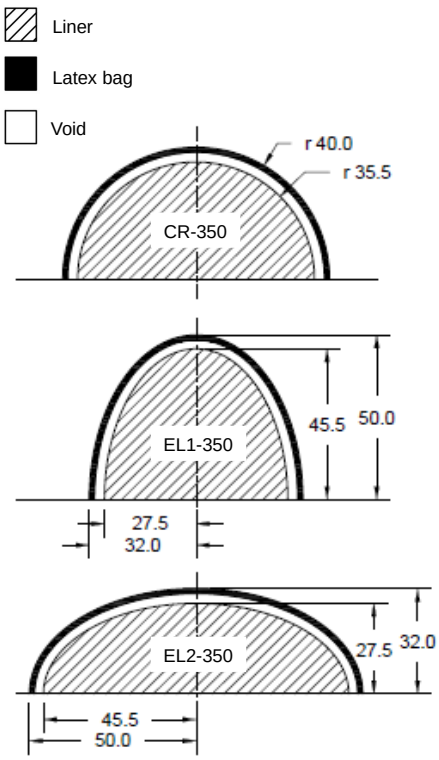

b) Cross sections (note latex bag is 1.5mm thick)

Figure 2: Schematic of centrifuge test apparatus.

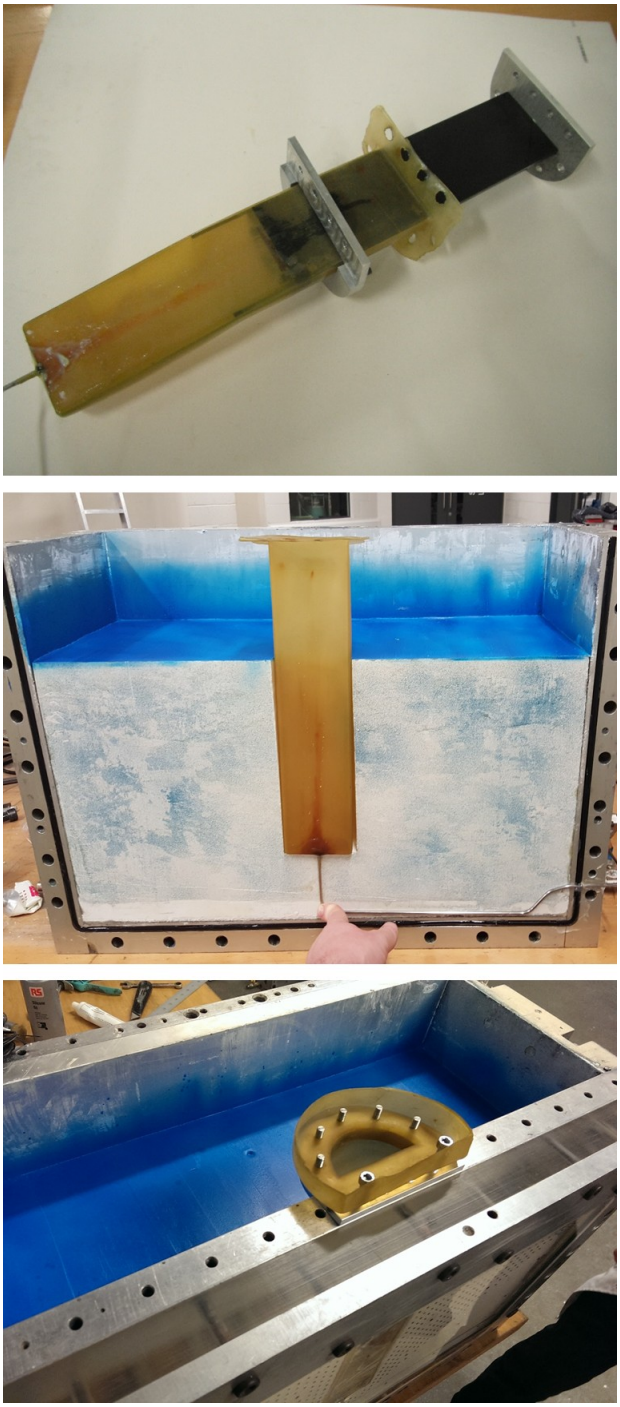

Figure 3: Photographs of apparatus showing: (top) assembly of former, latex bag and bracket, (middle) location of apparatus within the soil model, (bottom) attachment of the apparatus to the model box**.**

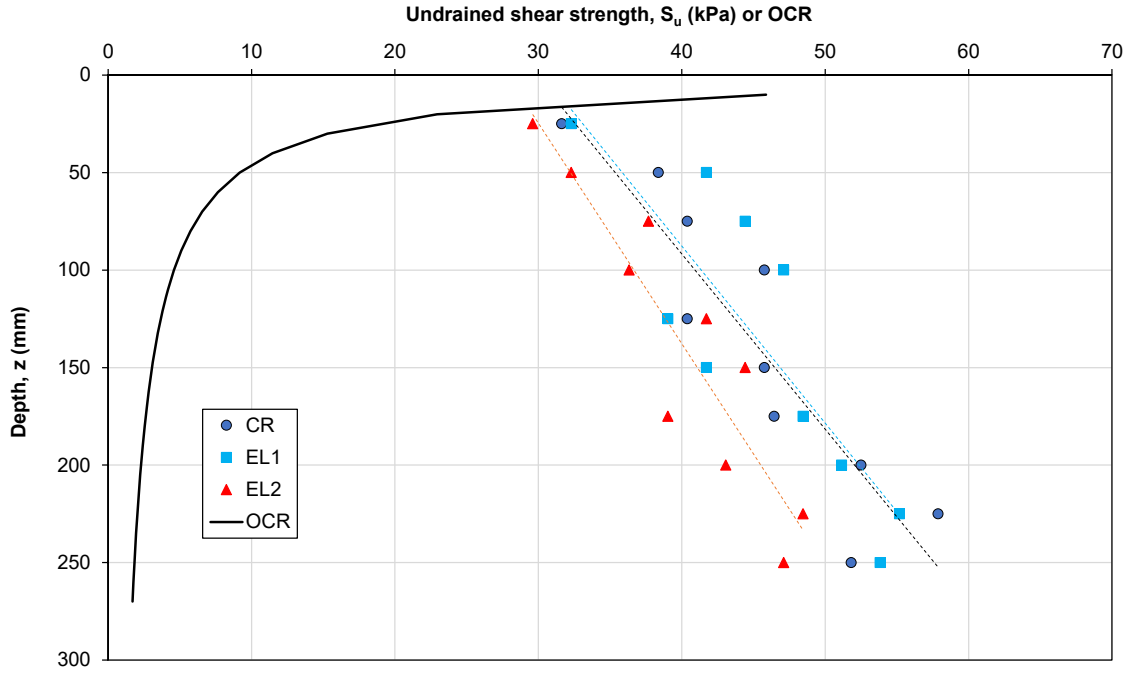

Figure 4: Undrained shear strength and OCR with depth for CR, EL1 and EL2.

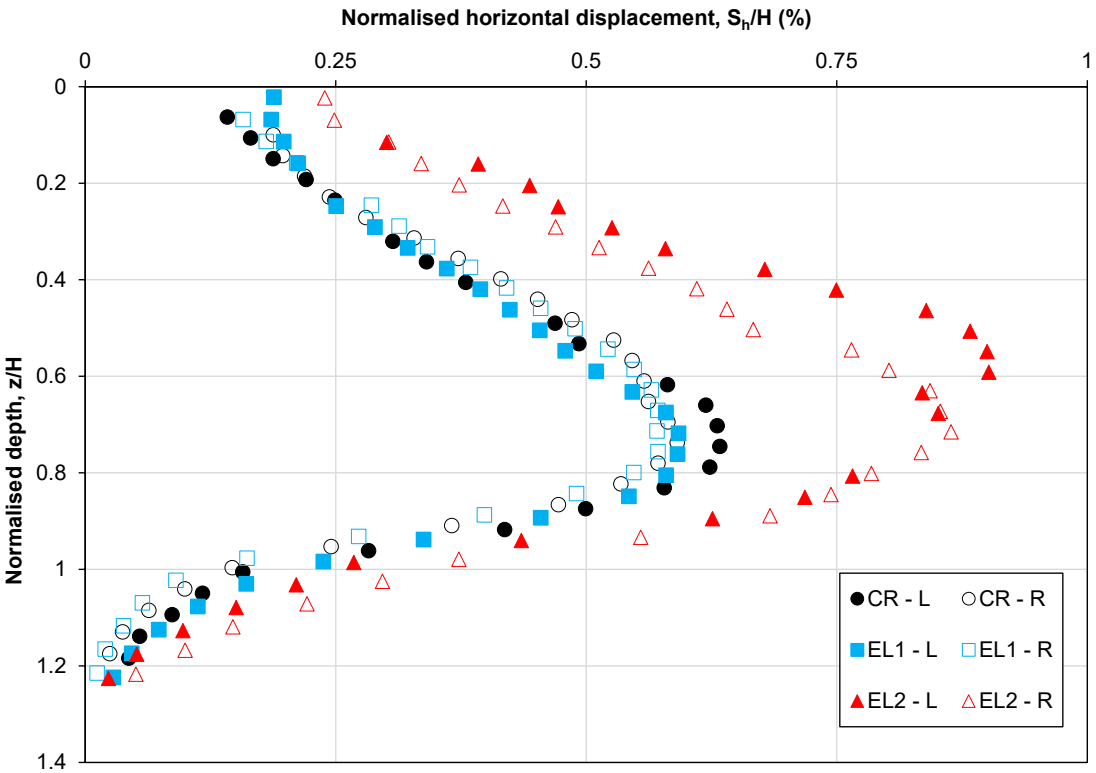

Figure 5: Horizontal displacement with depth for CR, EL1 and EL2 (L: results from left side of model, R: results from right side).

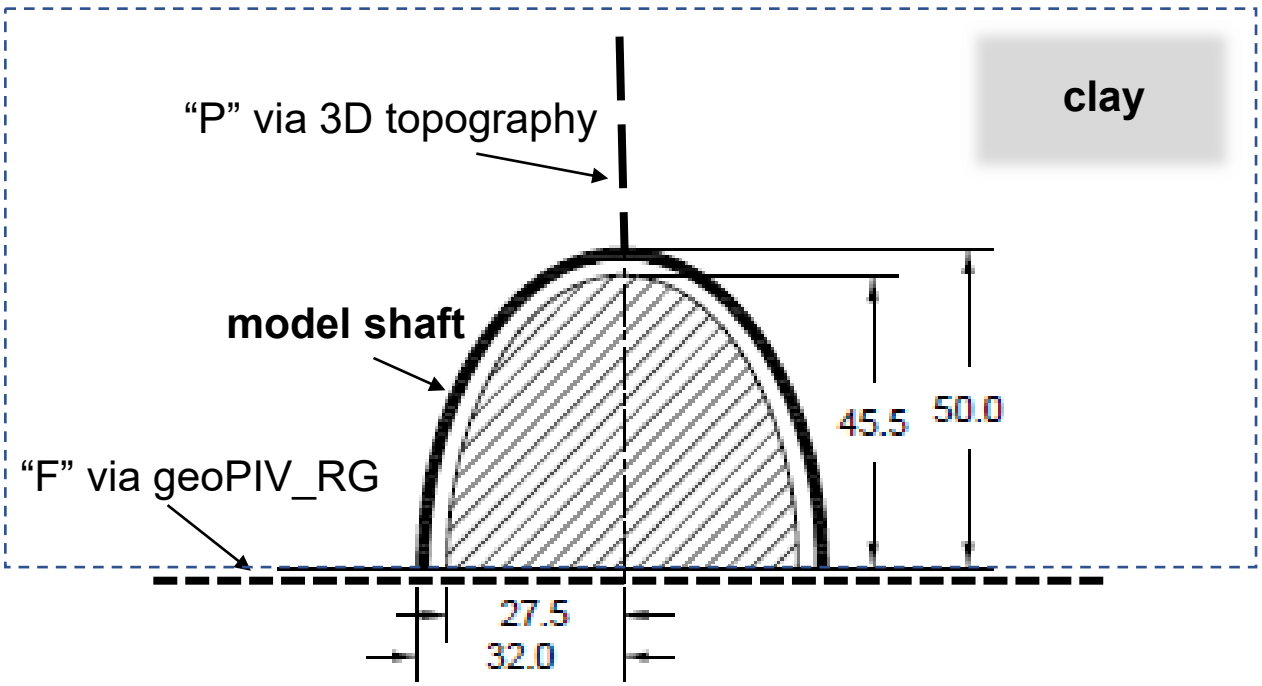

EL1

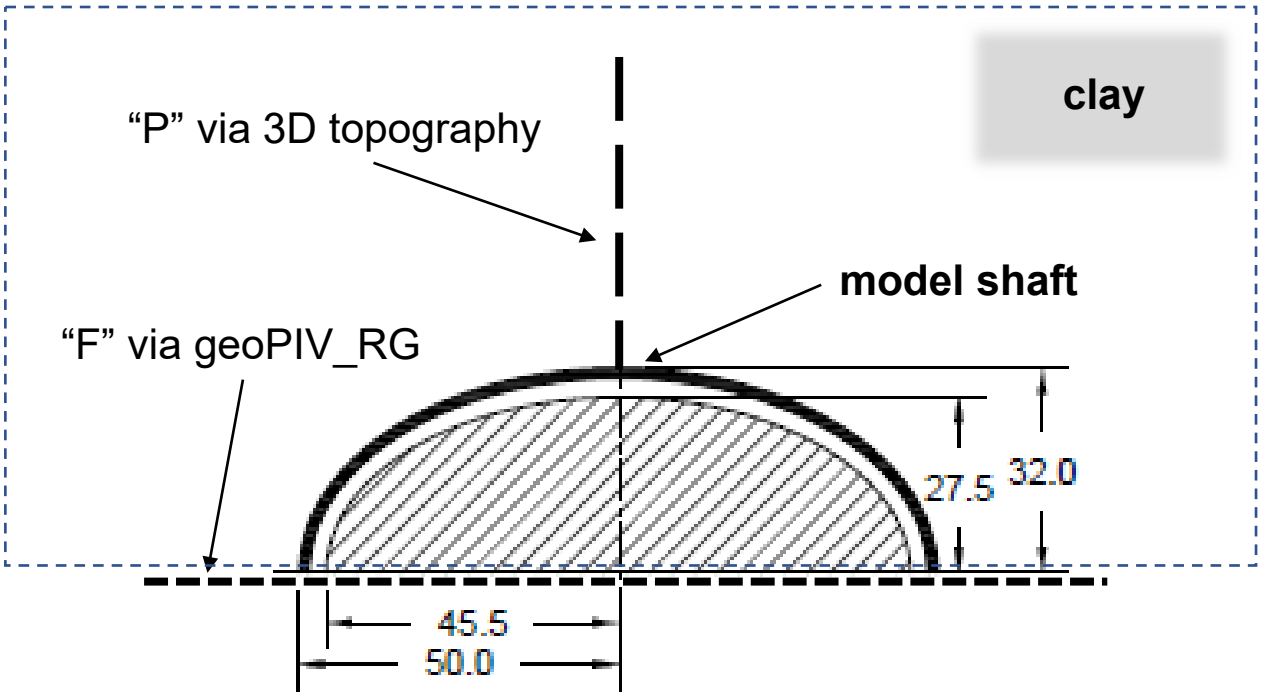

EL2

Figure 6: Sketch to show measurement locations

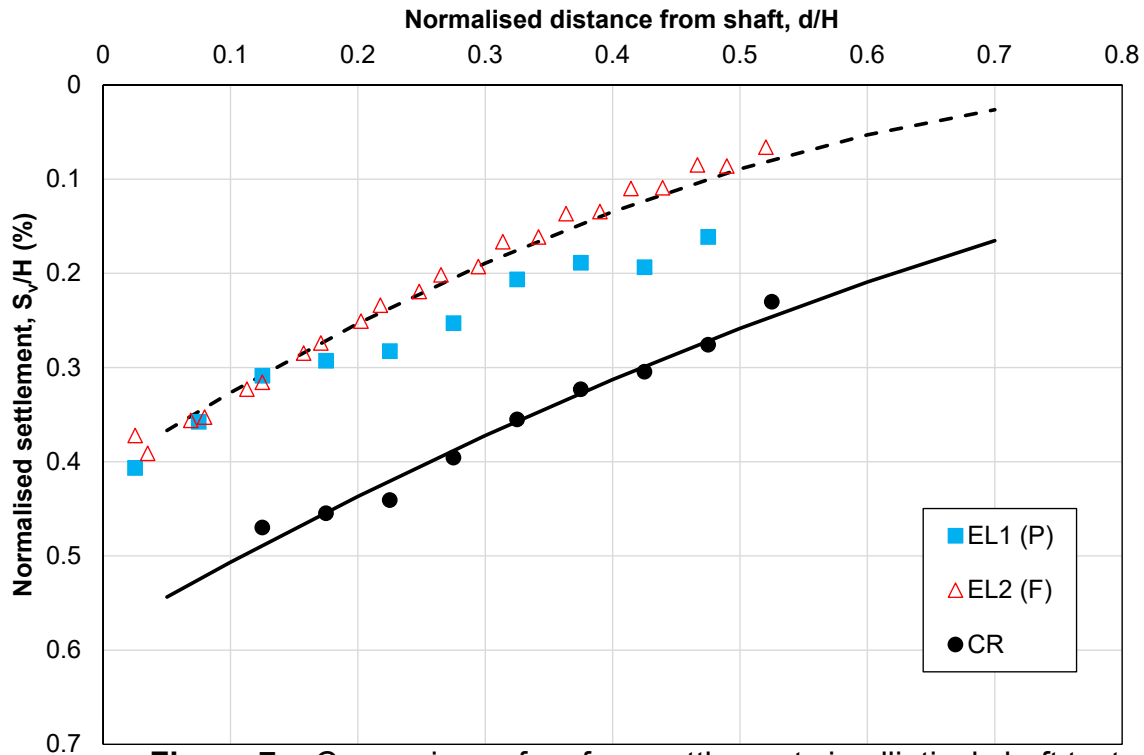

Figure 7a: Comparison of surface settlements in elliptical shaft test (EL) along the major axis direction with reference circular shaft data (CR).

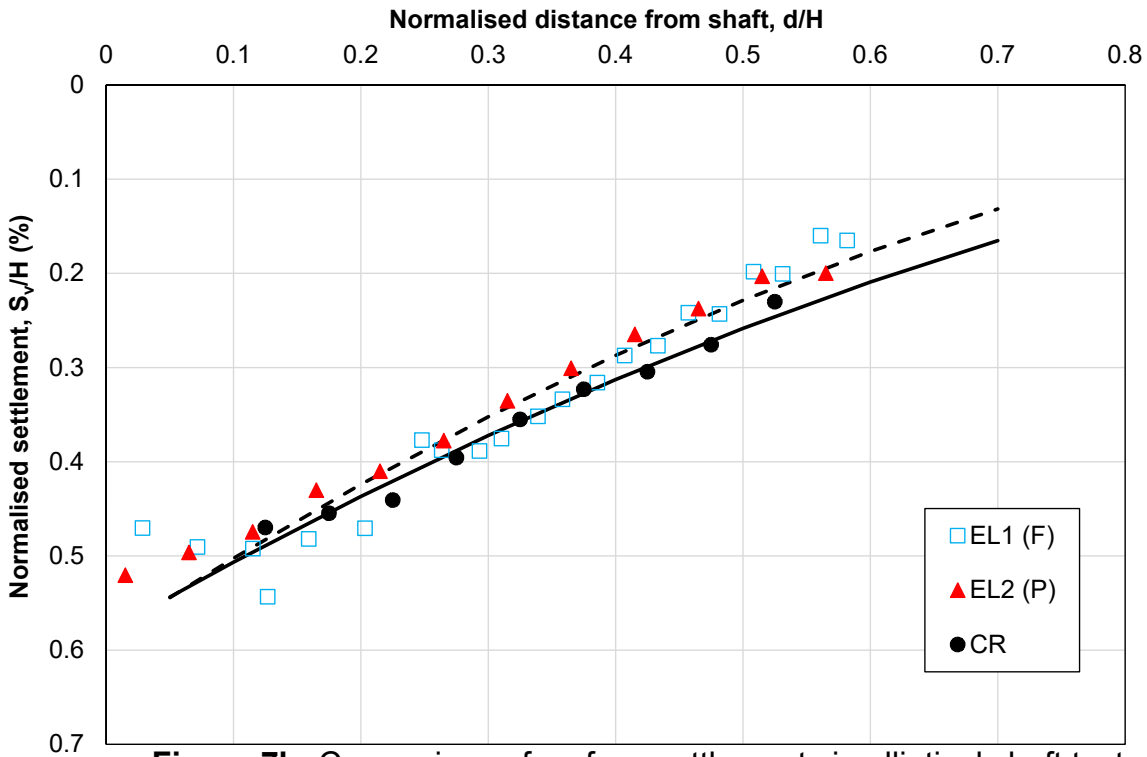

Figure 7b: Comparison of surface settlements in elliptical shaft test (EL) along the minor axis direction with reference circular shaft data (CR).

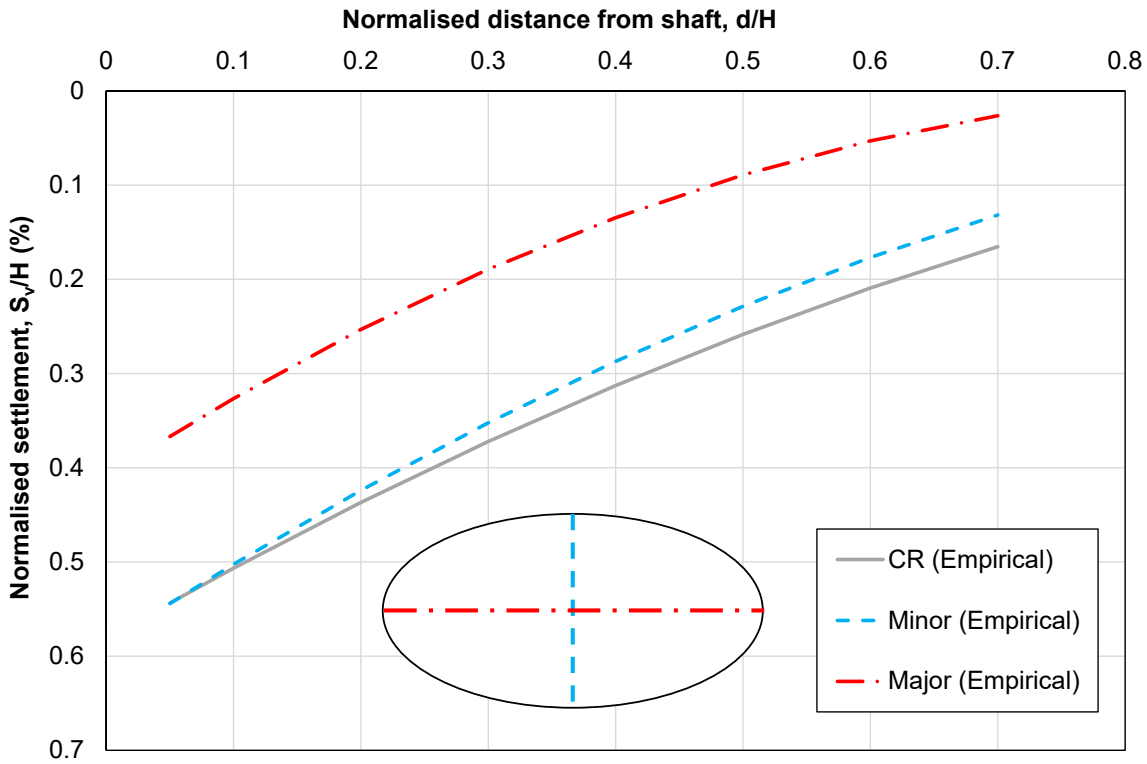

Figure 8: Design lines for surface settlements arising for elliptical shaft construction in clay.

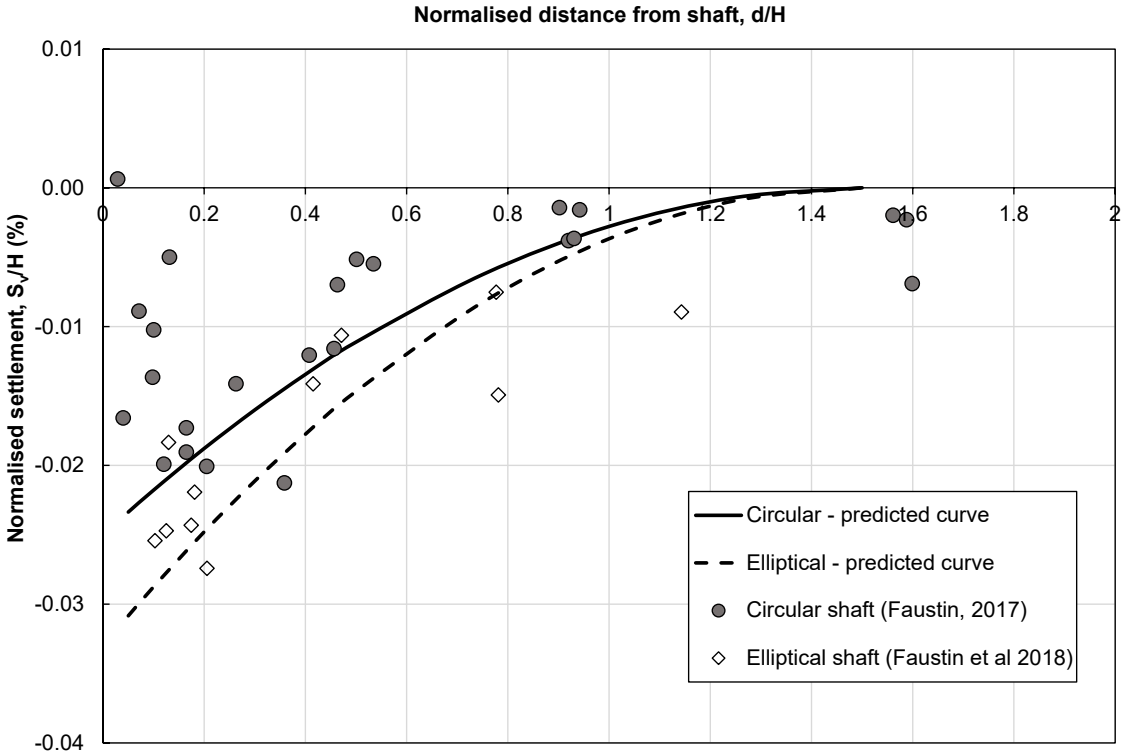

Figure 9: Comparison of Equation 2 with the results of Faustin (after Faustin *et al.*, 2018)